

Venkatachalam Taracad (Orcid ID: 0000-0001-9747-1105)

Bhalla Rajiv (Orcid ID: 0000-0003-1421-3667)

Lawrie Ken (Orcid ID: 0000-0002-8061-3696)

Synthesis of ^{18}F -radiolabeled diphenyl gallium dithiosemicarbazone using a novel halogen exchange method and in vivo biodistribution.#

T.K. Venkatachalam*¹, D.H.R. Stimson¹, R. Bhalla¹, K. Mardon¹, Paul.V. Bernhardt², D.C. Reutens¹

¹Centre for Advanced Imaging and ²School of Chemistry and Molecular Biosciences, The University of Queensland, Brisbane 4072.

*Corresponding Author: t.venkatachalam@uq.edu.au

Abstract:

^{18}F -radiolabeled diphenyl gallium thiosemicarbazone was prepared by [^{18}F] fluoride exchange of a nitrate anion under mild conditions. The diphenyl gallium thiosemicarbazone chloride is easily prepared in gram quantities and can be used at room temperature in the presence of oxygen. The corresponding nitrate complex is prepared using silver nitrate in methanol solvent and can be stored under nitrogen for weeks before radiolabeling. The biodistribution of this new tracer was studied in mice using Positron Emission Tomography (PET).

Keywords: Synthesis, gallium, dithiosemicarbazone, radiochemistry, biodistribution.

This paper is dedicated to Prof. Leone Spiccia (Monash University, Australia) a friend, scholar and mentor for his dedicated and tireless contribution to science.

This article has been accepted for publication and undergone full peer review but has not been through the copyediting, typesetting, pagination and proofreading process which may lead to differences between this version and the Version of Record. Please cite this article as doi: 10.1002/jlcr.3746

Introduction:

Thiosemicarbazones and semicarbazones can coordinate with many metal ions because of the presence of several donor atoms such as nitrogen, oxygen and sulphur in their structural core.

The preparation and characterization of diversely substituted thiosemicarbazones and semicarbazones has been explored since the 1950s¹ and extensive studies of coordination compounds with metal ions were undertaken in the following decade². Lobana et al.³ have compiled a detailed review of the bonding and structural characteristics of thiosemicarbazones and reported strategies to prepare new derivatives. Several workers in the past³⁻¹¹ have explored the possibility of introducing various metal ions in the core structure of thiosemicarbazone and extensively studied their structure and biological activity.

Dithiosemicarbazones readily coordinate 3d-transition metal ions¹²⁻²⁴ and have been used to chelate positron emitting isotopes such as copper-64 and gallium-68²⁵⁻³⁰. Pascu et al.^{8,31-33} synthesized a variety of ⁶⁸Ga-complexes of dithiosemicarbazone as potential imaging agents.

Pascu et al.³¹ also used a transmetallation strategy to radiolabel zinc complexes of dithiosemicarbazones with ⁶⁴Cu. This was accomplished with an aim to use the probe in hypoxia related imaging modality. Furthermore, the authors indicated that their strategy could serve as target specific site in vivo imaging studies. Since ¹⁸F is more widely available than ⁶⁴Cu and has a longer half-life than ⁶⁸Ga, we sought a facile method to introduce ¹⁸F in the core structure of gallium complexes of dithiosemicarbazones and explored whether Ga-¹⁸F dithiosemicarbazone complexes can be potentially used for *in vivo* imaging. These compounds form a square pyramidal structure, raising the possibility of introducing positron emitting isotopes easily using a halogen exchange strategy. Although this method of introducing fluorine-18 has been explored by McBride et al.³⁴⁻³⁹ and Bhalla et al.⁴⁰⁻⁴³ using different metal chelate moieties, the complexes generated by these groups are all hydrophilic. In contrast, gallium-¹⁸F complexes of dithiosemicarbazones will be both lipophilic and neutral. We

recently reported ⁴⁴ a process for introducing [¹⁸F]fluoride into the core structure of dithiosemicarbazones using a halogen exchange method under mild conditions. Here, we describe semi-automated synthesis of this radiotracer, which includes the purification of the tracer and report its biodistribution in mice.

Experimental:

All chemicals were obtained from Sigma Aldrich and used without further purification. Anhydrous methanol and dimethyl sulfoxide also obtained from Sigma Aldrich were stored under nitrogen and transferred into flasks for synthesis under nitrogen atmosphere to eliminate any moisture. Sodium methoxide was also kept and transferred under nitrogen atmosphere. Synthesis of the gallium chloro dithiosemicarbazone, its characterization along and initial radiolabeling studies have been reported earlier ⁴⁴.

Preparation of gallium nitrate dithiosemicarbazone: In a scintillation vial was placed 20 mg of the red complex of gallium chloro dithiosemicarbazone, into which was syringed in 10 mL of anhydrous methanol under nitrogen atmosphere. The contents were allowed to stir for 10 min; the complex did not dissolve at this stage. To the suspension was added carefully 8 mg of solid silver nitrate and the contents of the flask manually shaken for 3 min and stirred vigorously for another 10 min, when the solution turned a reddish yellow color and a white precipitate of silver chloride was seen (Note: Manual shaking was found to be essential to initiate the reaction due to heterogeneity of the reaction medium). The contents of the scintillation vial were then transferred into a 20 mL centrifuge tube under nitrogen and centrifuged at 3000 rpm for 5 min. A 0.5 mL aliquot of the orange/yellow supernatant was transferred into a 10 mL glass vial and the solvent evaporated under nitrogen to obtain an orange/yellow residue. After thorough drying of the residue, the vial was crimp-capped with a

butyl rubber closure. This intermediate reactive nitrate complex could be stored under these conditions for several days without adversely affecting radiolabeling.

Radiolabeling of the precursor: A reproducible method was achieved after several trials and the detailed steps are described below.

Production of fluorine-18: No-carrier-added fluorine-18 was manufactured via the $^{18}\text{O}(\text{p},\text{n})^{18}\text{F}$ nuclear reaction using a *Cyclone® 18 Twin* (IBA, Belgium) dual ion source cyclotron. Approximately 0.7 mL of pure water enriched to >98% [^{18}O] H_2O was irradiated with 18 MeV protons at a beam current of 14 μA for up to 30 min producing up to 30 GBq of fluorine-18. The aqueous [^{18}F] F^- was transferred from the cyclotron target to a 10 mL glass receiving vial located in a hot-cell via 1.6 mm diameter (OD) polypropylene tubing approximately 20 m in length under helium pressure. The receiving vial was measured for radioactive content in a dose calibrator housed within the hot-cell before delivery into a lead pot. The lead pot was then manually transferred to a fume cabinet where aliquots of the aqueous [^{18}F] F^- were taken for radiolabeling.

Analytical HPLC conditions for determination of radiolabeled compound: HPLC analysis was performed using a Shimadzu model *LC 20AD* instrument with a diode array detector, a quaternary pump, thermostated column compartment, and a radio detector (Bioscan *Flow Count* with a pin-diode detector) in conjunction with a *LCsolutions* software computer operated system. The analytical column used was a *ZORBAX Eclipse Plus C18* (Agilent) of dimensions 4.6 X 150 mm, 5 μm . The temperature of the column was maintained at 30°C during the analysis. The eluent used was a mixture of 0.1% TFA in water (A) and Acetonitrile (B) under gradient conditions of 10 - 90% B over 30 min. The flow rate employed was 1 mL/min and the injection volume were 20 μL . Under these experimental conditions, the radiolabeled compound eluted at 15.6 min.

Preparation of [^{18}F] fluoride / $\text{K}_{222}/\text{K}_2\text{CO}_3$: All manual operations were performed behind lead blocks arranged within protective biological safety cabinets and employing Personal Protective Equipment (PPE). To dry the [^{18}F] F^- , 1.9 mg (5 μmol) of Kryptofix® 222 (K_{222}) was first dissolved in 0.5 mL of dry acetonitrile and transferred into a 10 mL glass Wheaton vial. To this was added 25 μL of 0.1 M K_2CO_3 (2.5 μmol) followed by 100 μL of the [^{18}O] H_2O containing cyclotron-produced [^{18}F] F^- (typically 200-300 MBq). The vial was septum capped, placed in a dry block heater maintained at 100°C and heated under nitrogen making sure that the azeotropic evaporation of the solvent took place smoothly without bumping or spurting. Evaporation was continued for approximately 20 min resulting into a dry solid mixture of [^{18}F] $\text{F}^-/\text{K}_{222}/\text{K}_2\text{CO}_3$.

Radiolabeling protocol: The vial containing [^{18}F] $\text{F}^-/\text{K}_{222}/\text{K}_2\text{CO}_3$ was removed from the heater and set aside while the heating block was cooled to 45°C using compressed air flow. The gallium nitrate dithiosemicarbazone was dissolved in anhydrous dimethyl sulfoxide (500 μL) resulting in a light yellow-orange solution. The solution was transferred, using a dry syringe previously flushed with nitrogen, to the vial containing [^{18}F] $\text{F}^-/\text{K}_{222}/\text{K}_2\text{CO}_3$ and a red-orange colored solution resulted. The vial was then placed in the heater block at 45°C and allowed to react for 3 min. The crude reaction mixture was further purified and reformulated using the *Synthra* automated module.

Purification of labeled crude reaction mixture: Purification used a combination of semi-preparative HPLC and Solid Phase Extraction (SPE) using a pre-programmed automated sequence in a *Synthra* radiosynthesis module (*Synthra GmbH*, Hamburg, Germany) housed within a hot-cell (*Tema Sinergie*, Faenza, Italy). To separate the radiolabeled compound from the starting material, HPLC was performed using a *ZORBAX Eclipse XDB-C18* 250 x 10 mm semi-preparative column (*Agilent*, Santa Clara, Ca) and a mixture of 1% trifluoroacetic acid in water/acetonitrile (65:35) as the eluent. Chromatographic separation was achieved isocratically

at a flow rate of 4 mL/min. Radiation and UV detection at 254 nm were used to identify the product. The SPE cartridge used was a *Waters C-18 Plus Sep-Pak* (Waters Corporation, Milford, Ma) preconditioned with 10 mL of ethanol and 10 mL of water followed by drying with air.

The crude product mixture was syringed out using a disposable syringe and diluted to 1 mL in water (approximately 50% dilution). The syringe was connected manually to position 3 of the syringe valve of the Synthra module (see Figure 1). In the automated sequence program, the solution was injected into the 3 mL HPLC loop and peak collection at approximately 14 min was achieved using the Synthra module's peak-cut feature. The product was then transferred into a vial containing 30 mL of water and the contents stirred for 5 min before being transferred onto the preconditioned SPE cartridge via valve 35 with the solution directed to waste (via valve 36). The SPE cartridge was then washed with 10 mL of water from vial C3. The product was then eluted from the SPE cartridge using 1.0 mL of ethanol supplied from vial C2 and directed to the product vial via valve 36. The product vial was housed in a lead container ready for collection. The product was then removed from the synthesizer and subjected to QC analysis by analytical HPLC.

Animal studies: The biodistribution of the tracer was examined in mice. All studies were approved by the Animal Ethics Committee of The University of Queensland in accordance with the Australian Code for the Care and Use of Animals for Scientific Purposes.

PET/CT imaging protocol: Four healthy C57BL6J female mice aged 12 weeks were anaesthetized with 2% isoflurane (IsoFlo, Abbott Laboratories) in a closed anesthetic induction chamber. Animals were monitored using ocular and pedal reflexes to ensure deep anesthesia. Anaesthetized mice, with a cannulated tail vein, were placed in an Inveon PET/CT scanner (Siemens). Physiological monitoring was performed using an animal monitoring system (the

BioVet™ system, m2m Imaging, Australia). Mice were injected with approximately 5 MBq of ¹⁸F-fluoro-diphenyl gallium dithiosemicarbazone solution in a volume of 150 μL via the tail vein catheter in a slow bolus injection.

Dynamic PET data acquisition was performed for 60 min. The emission data were normalized and corrected for decay and dead volume. The list-mode data were sorted into 54 dynamic frames (12 x 10 s, 16 x 30 s, 20 x 60 s, 6 x 300 s time frames). The resulting sinograms were reconstructed using a filtered back-projection and an ordered-subset expectation maximization (OSEM2D) algorithm and analyzed using the Inveon Research Workplace software (IRW, Siemens). Following the PET scans, the CT images of the mice were acquired through an X-ray source with the voltage set to 80 kV and the current set to 500 μA. The scans were performed using 360° rotation with 120 rotation steps with a low magnification and a binning factor of four. The exposure time was 230 ms with an effective pixel size of 106 μm. The total CT scanning process took approximately 15 min. The CT images were reconstructed using Feldkamp reconstruction software (Siemens). CT and PET datasets of each individual animal were aligned using IRW software (Siemens) to ensure good overlap of the organs of interest. Using morphologic CT information, three dimensional regions of interest were placed over the whole body, as well as individual organs of interest including the heart, kidney, lungs, liver, and brain. Activity per voxel was converted to nCi/mL using a conversion factor obtained by scanning a cylindrical phantom with a solution containing fluorine-18 of known activity to account for PET scanner efficiency. Activity concentrations were then expressed as the percentage of the decay-corrected, injected activity per cm³ of tissue, approximated as percentage injected dose/g of tissue (%ID/g). At the end of the imaging sessions, the mice were sacrificed, and the organs were surgically removed, weighed and placed in tubes. The tubes were counted using a gamma counter (Perkin Elmer, Model 2480, Gamma Counter Wizard 2,

Illinois, USA) and the results were expressed as % injected dose/g organ and % injected dose/organ to confirm the data obtained with the PET/CT imaging study.

Results and Discussion:

Synthesis of gallium diphenyl dithiosemicarbazone chloride was achieved using a previously published procedure^{45,46}. The diphenyl thiosemicarbazone was treated with sodium methoxide in anhydrous methanol followed by the addition of a stoichiometric amount of gallium chloride pre-dissolved in anhydrous methanol as shown in Scheme 1.

Subsequently, an exchange reaction was conducted to replace the chloride with nitrate, a better leaving group. The heterogeneous phase transfer methodology using silver nitrate in methanol is shown in Scheme 2. The nitrate complex obtained was further treated with [¹⁸F]F⁻ in a subsequent exchange to obtain the ¹⁸F-radiolabeled gallium complex of diphenyl dithiosemicarbazone. HPLC purification and reformulation of the tracer was achieved by using a Synthra automated module. Figure 1 shows the Graphical User Interface (GUI) of the Synthra automated module used for the HPLC purification of the crude reaction mixture and subsequent reformulation. As can be seen from figure 1 that certain alterations in the synthetic module for the purification of the final radiolabeled compound was necessary. As explained before, radio labelling was performed manually using heterogenous reaction of silver nitrate and gallium ligand followed by reaction with ¹⁸F, this modification was essential. In other words, the whole synthesis and purification was achieved using a semi-automated process.

The analytical HPLC chromatogram of the radiolabeled compound is shown in Figure 2. The initial peak in the radio chromatogram is the [¹⁸F]F⁻ followed by the second peak at 15.5 min, corresponding to the radiolabeled product. The figures also depict the UV peak obtained for the product. Caution should be exercised here not to mistake the large UV peak in the chromatogram at 15-16 min for non-radioactive ¹⁹F-labelled gallium diphenyl dithiosemicarbazone since under our experimental conditions, the retention time of the starting

chloro- compound and the fluorine labelled complex was identical. Presumably, UV peak of the ^{19}F -labelled diphenyl gallium dithiosemicarbazone is very close to the unreacted chloro- compound (see figure 2, lower panel). The semi preparative chromatogram is shown in Figure

3. The radioactive peak at 14 min was collected and was used for animal studies.

The QC analytical HPLC (Figure 4) shows that a clean ^{18}F -radiolabeled diphenyl gallium thiosemicarbazone complex was obtained at 15.3 min. The accompanying UV trace shows that there are three peaks around that range. The second large peak has a shoulder peak at approximately 15.25 min which we believe corresponds to the ^{19}F -complex. Radiosynthesis was repeated several times without difficulty and the radiochemical yield of each trial is reported in Table 1. Ongoing work aims to enhance radiochemical yield.

In order to confirm the stability of the complex, the same batch radiolabeled complex used for *vivo* studies was further evaluated for its stability. Figure 5 shows the HPLC chromatogram of the complex after 2 hours of post injection. It is evident from the figure that the HPLC profile showed no sign of decomposition of the complex demonstrating the stability of the radiotracer under our experimental conditions. The absence of uptake in bone also confirms the stability of this radiotracer.

Stability of the intermediate nitrate complex: The nitrate complex was stable when stored as a solid under nitrogen atmosphere in a sealed vial. Aliquots from a single batch of the complex stored under nitrogen atmosphere for weeks could be radiolabeled without difficulty.

Homogenous solution exchange with silver triflate: We also examined the use of silver triflate as the homogenous exchange medium (Scheme 3). Silver triflate is soluble in organic solvents whereas silver nitrate is insoluble in methanol. Although we were able to radiolabel the compound, the yield of the product was considerably lower, perhaps due to the high reactivity of the triflate for trace amounts of water in the solvents. It is possible that less-reactive silver

salts like tosylate could improve this exchange methodology and it may be possible to use other metal salts for future applications.

Biodistribution of ^{18}F -diphenylgalliumdithiosemicarbazone: The biodistribution is similar to that of blood flow tracers pyruvaldehyde bithiosemicarbazone copper complexes ⁴⁷. PET/CT images of tracer uptake in a single mouse are shown in Figure 6.

Time activity curve obtained from healthy C57BL6J mice injected with ^{18}F -thiosemicarbazone is shown in Figure 7. At 60 min, the highest uptake was seen in the liver followed by the heart, kidney, gut and brain. Rapid uptake (peak uptake approximately 2 min) with an injected dose/gram of 2 to 30% was observed in individual organs including the brain, the latter suggesting that the tracer crosses the blood-brain barrier. Other researchers have described that pyruvaldehyde bithiosemicarbazone copper complexes efficiently crosses the blood brain barrier ^{15,27,28,45,46,48}. Most notably, no significant radioactivity was observed in bone, which suggests that the Ga-fluoride bond is stable *in vivo*. Biodistribution at 60 min is presented in Table 2 and is consistent with the dynamic imaging data.

Conclusions:

This research builds on the use of complexes of group-13 metals to form high affinity complexes with [^{18}F]fluoride ⁴⁹, driven with a goal for the development of lipophilic radiolabeled complexes which may have applications of neuroimaging. Whilst Bhalla et al.⁴⁰⁻⁴² reported the preparation of the first Ga- ^{18}F complexes, they did not report the properties of their complexes *in vivo*. This paper describes the first example of *in vivo* imaging of a Ga- ^{18}F compound. Furthermore, our studies demonstrate that the Ga- ^{18}F bond is stable *in vivo* with our thiosemicarbazone ligand. Whilst our current yields are low, the stability of the Ga- ^{18}F bond *in vivo* suggests that Ga- ^{18}F complexes of other derivatives of thiosemicarbazones and of other chelate frameworks should be explored.

Acknowledgements: The research was funded in part by the Australian Research Council

Linkage Grant #LP130100703.

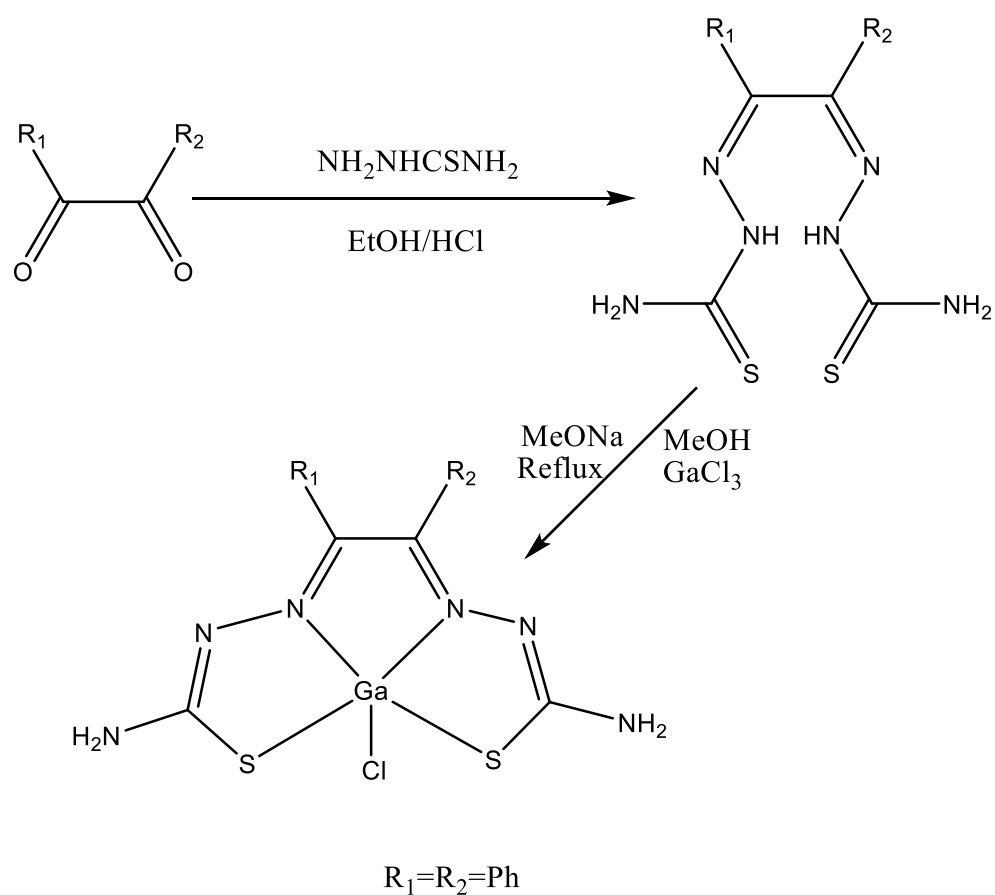
References

1. Bernstein J, Yale HL, Losee K, Holsing M, Martins J, Lott W. The Chemotherapy of Experimental Tuberculosis. III. The Synthesis of Thiosemicarbazones and Related Compounds1, 2. *Journal of the American Chemical Society*. 1951;73(3):906-912.
2. Gingras B, Somorjai R, Bayley C. The preparation of some thiosemicarbazones and their copper complexes. *Canadian Journal of Chemistry*. 1961;39(5):973-985.
3. Lobana TS, Sharma R, Bawa G, Khanna S. Bonding and structure trends of thiosemicarbazone derivatives of metals—an overview. *Coordination Chemistry Reviews*. 2009;253(7):977-1055.
4. Antholine WE, Knight JM, Petering DH. Inhibition of tumor cell transplantability by iron and copper complexes of 5-substituted 2-formylpyridine thiosemicarbazones. *Journal of medicinal chemistry*. 1976;19(2):339-341.
5. Bröckman R, Thompson J, Bell M, Skipper H. The carcinostatic activity of α -(N)-heterocyclic carboxaldehyde thiosemicarbazone. *Cancer Res*. 1956;16:167-169.
6. Donnelly PS. The role of coordination chemistry in the development of copper and rhenium radiopharmaceuticals. *Dalton Transactions*. 2011;40(5):999-1010.
7. Jensen K. Thiosemicarbazidverbindungen des zweiwertigen Palladiums und Platins. *Zeitschrift für anorganische und allgemeine Chemie*. 1934;221(1):6-10.
8. Jensen K. Zur Stereochemie des koordinativ vierwertigen Nickels. *Zeitschrift für anorganische und allgemeine Chemie*. 1936;229(3):265-281.
9. Kalinowski DS, Yu Y, Sharpe PC, et al. Design, synthesis, and characterization of novel iron chelators: Structure– activity relationships of the 2-benzoylpyridine thiosemicarbazone series and their 3-nitrobenzoyl analogues as potent antitumor agents. *Journal of medicinal chemistry*. 2007;50(15):3716-3729.
10. Turk SR, Shipman Jr C, Drach JC. Structure-activity relationships among α -(N)-heterocyclic acyl thiosemicarbazones and related compounds as inhibitors of herpes simplex virus type 1-specified ribonucleoside diphosphate reductase. *Journal of general virology*. 1986;67(8):1625-1632.
11. West DX, Liberta AE, Padhye SB, et al. Thiosemicarbazone complexes of copper (II): structural and biological studies. *Coordination Chemistry Reviews*. 1993;123(1-2):49-71.
12. Bermejo E, Castiñeiras A, García-Santos I, Fostiak LM, Swearingen JK, West DX. Spectral and Structural Studies of Transition Metal Complexes of 2-Pyridineformamide N (4)-ethylthiosemicarbazone. *Zeitschrift für anorganische und allgemeine Chemie*. 2005;631(4):728-738.
13. Booth BA, Agrawal KC, Moore EC, Sartorelli AC. α -(N)-Heterocyclic Carboxaldehyde Thiosemicarbazone Inhibitors of Ribonucleoside Diphosphate Reductase. *Cancer research*. 1974;34(6):1308-1314.
14. Castiñeiras A, Garcia I, Bermejo E, West DX. Structural and spectral studies of 2-pyridineformamide thiosemicarbazone and its complexes prepared with zinc halides. *Zeitschrift für Naturforschung B*. 2000;55(6):511-518.
15. Cutler CS, Giron MC, Reichert DE, et al. Evaluation of gallium-68 tris (2-mercaptobenzyl) amine: a complex with brain and myocardial uptake. *Nuclear medicine and biology*. 1999;26(3):305-316.

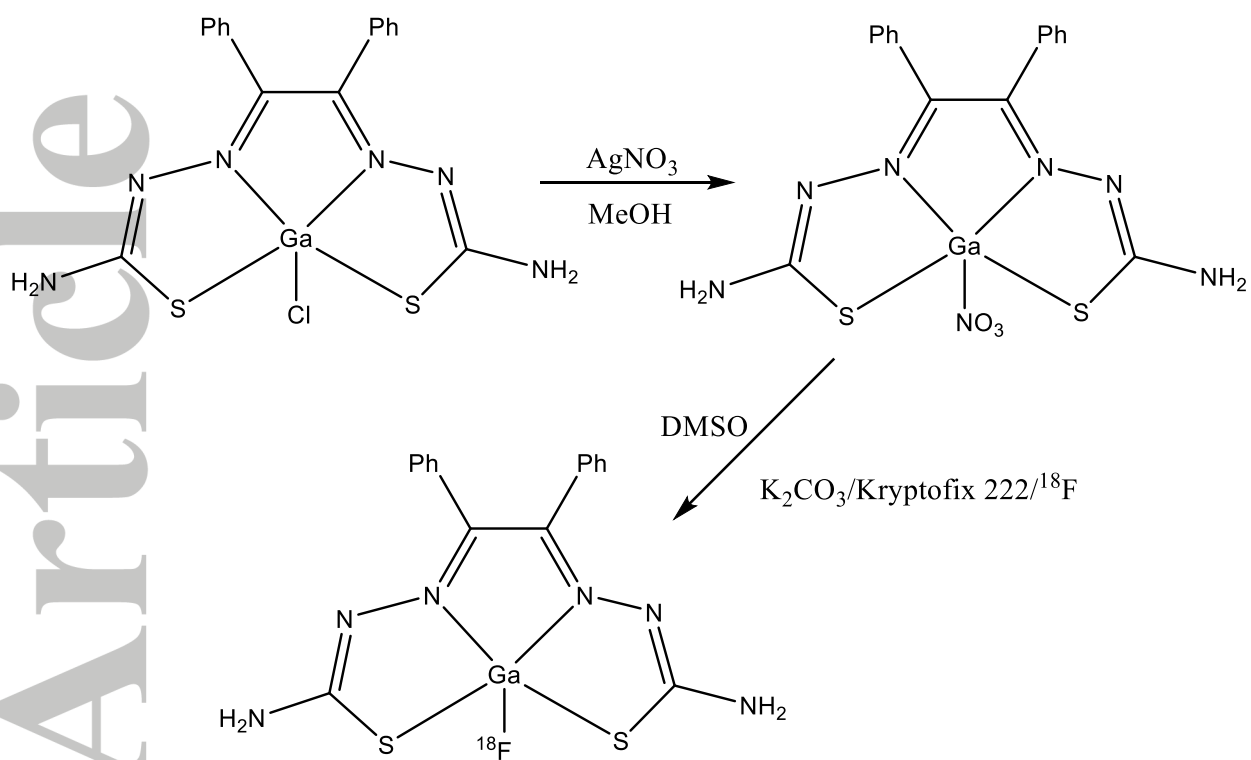
16. Easmon J, Pürstinger G, Heinisch G, et al. Synthesis, cytotoxicity, and antitumor activity of copper (II) and iron (II) complexes of 4 N-azabicyclo [3.2. 2] nonane thiosemicarbazones derived from acyl diazines. *Journal of medicinal chemistry*. 2001;44(13):2164-2171.
17. Graminha AE, Vilhena FS, Batista AA, et al. 2-Pyridiniformamide-derived thiosemicarbazones and their iron (III) complexes: Potential antineoplastic activity. *Polyhedron*. 2008;27(2):547-551.
18. Jagadeesh M, Kumar VA, Ramachandiraiah C, Reddy AV. New Halogenated Thiosemicarbazones as Potential Antimicrobial Agents: synthesis and spectral characterization. 2013.
19. Kowol CR, Trondl R, Heffeter P, et al. Impact of metal coordination on cytotoxicity of 3-aminopyridine-2-carboxaldehyde thiosemicarbazone (triapine) and novel insights into terminal dimethylation. *Journal of medicinal chemistry*. 2009;52(16):5032-5043.
20. Mendes IC, Moreira JP, Ardisson JD, et al. Organotin (IV) complexes of 2-pyridineformamide-derived thiosemicarbazones: antimicrobial and cytotoxic effects. *European journal of medicinal chemistry*. 2008;43(7):1454-1461.
21. Mendes IC, Soares MA, dos Santos RG, Pinheiro C, Beraldo H. Gallium (III) complexes of 2-pyridineformamide thiosemicarbazones: cytotoxic activity against malignant glioblastoma. *European journal of medicinal chemistry*. 2009;44(5):1870-1877.
22. West DX, Swearingen JK, Valdés-Martínez J, et al. Spectral and structural studies of iron (III), cobalt (II, III) and nickel (II) complexes of 2-pyridineformamide N (4)-methylthiosemicarbazone. *Polyhedron*. 1999;18(22):2919-2929.
23. Yu Y, Kalinowski DS, Kovacevic Z, et al. Thiosemicarbazones from the old to new: iron chelators that are more than just ribonucleotide reductase inhibitors. *Journal of medicinal chemistry*. 2009;52(17):5271-5294.
24. Zeglis BM, Divilov V, Lewis JS. Role of metalation in the topoisomerase II α inhibition and antiproliferation activity of a series of α -heterocyclic-N4-substituted thiosemicarbazones and their Cu (II) complexes. *Journal of medicinal chemistry*. 2011;54(7):2391-2398.
25. Dearling JL, Blower PJ. Redox-active metal complexes for imaging hypoxic tissues: structure–activity relationships in copper (II) bis (thiosemicarbazone) complexes. *Chemical Communications*. 1998(22):2531-2532.
26. Fujibayashi Y, Taniuchi H, Yonekura Y, Ohtani H. Copper-62-ATSM: a new hypoxia imaging agent with high membrane permeability and low redox potential. *The Journal of Nuclear Medicine*. 1997;38(7):1155.
27. Green MA, Klippenstein DL, Tennison JR. Copper (II) bis (thiosemicarbazone) complexes as potential tracers for evaluation of cerebral and myocardial blood flow with PET. *Journal of nuclear medicine*. 1988;29(9):1549-1557.
28. Green MA, Mathias CJ, Willis LR, et al. Assessment of Cu-ETS as a PET radiopharmaceutical for evaluation of regional renal perfusion. *Nuclear medicine and biology*. 2007;34(3):247-255.
29. Oh M, Tanaka T, Kobayashi M, et al. Radio-copper-labeled Cu-ATSM: an indicator of quiescent but clonogenic cells under mild hypoxia in a Lewis lung carcinoma model. *Nuclear medicine and biology*. 2009;36(4):419-426.
30. Vāvere AL, Lewis JS. Examining the relationship between Cu-ATSM hypoxia selectivity and fatty acid synthase expression in human prostate cancer cell lines. *Nuclear medicine and biology*. 2008;35(3):273-279.
31. Pascu SI, Waghorn PA, Conry TD, et al. Designing Zn (II) and Cu (II) derivatives as probes for in vitro fluorescence imaging. *Dalton Transactions*. 2007(43):4988-4997.

32. Pascu SI, Waghorn PA, Conry TD, et al. Cellular confocal fluorescence studies and cytotoxic activity of new Zn (II) bis (thiosemicarbazonato) complexes. *Dalton Transactions*. 2008(16):2107-2110.
33. Pascu SI, Waghorn PA, Kennedy BW, et al. Fluorescent copper (II) bis (thiosemicarbazones): synthesis, structures, electron paramagnetic resonance, radiolabeling, in vitro cytotoxicity and confocal fluorescence microscopy studies. *Chemistry—An Asian Journal*. 2010;5(3):506-519.
34. McBride WJ, D'Souza CA, Karacay H, Sharkey RM, Goldenberg DM. New lyophilized kit for rapid radiofluorination of peptides. *Bioconjugate chemistry*. 2012;23(3):538-547.
35. McBride WJ, D'Souza CA, Sharkey RM, et al. Improved 18F labeling of peptides with a fluoride-aluminum-chelate complex. *Bioconjugate chemistry*. 2010;21(7):1331-1340.
36. McBride WJ, Goldenberg DM, Sharkey RM. Al18F Labeling of Affibody Molecules. *Journal of Nuclear Medicine*. 2014;55(6):1043-1043.
37. McBride WJ, Sharkey RM, Karacay H, et al. A novel method of 18F radiolabeling for PET. *Journal of nuclear medicine*. 2009;50(6):991-998.
38. D'Souza CA, McBride WJ, Sharkey RM, Todaro LJ, Goldenberg DM. High-yielding aqueous 18F-labeling of peptides via Al18F chelation. *Bioconjugate chemistry*. 2011;22(9):1793-1803.
39. Lutje S, Franssen G, Sharkey R, et al. Anti-CEA antibody fragments labeled with [18F] AIF for PET imaging of CEA-Expressing Tumors. *Bioconjugate chemistry*. 2014;25(2):335-341.
40. Bhalla R, Burt J, Hector AL, et al. Complexes of aluminium, gallium and indium trifluorides with neutral oxygen donor ligands: Synthesis, properties and reactions. *Polyhedron*. 2016;106:65-74.
41. Bhalla R, Darby C, Levason W, et al. Triaza-macrocyclic complexes of aluminium, gallium and indium halides: fast 18 F and 19 F incorporation via halide exchange under mild conditions in aqueous solution. *Chemical Science*. 2014;5(1):381-391.
42. Bhalla R, Levason W, Luthra SK, McRobbie G, Sanderson G, Reid G. Radiofluorination of a Pre-formed Gallium (III) Aza-macrocyclic Complex: Towards Next-Generation Positron Emission Tomography (PET) Imaging Agents. *Chemistry-A European Journal*. 2015;21(12):4688-4694.
43. Glaser M, Iveson P, Hoppmann S, et al. Three methods for 18F labeling of the HER2-binding affibody molecule ZHER2: 2891 including preclinical assessment. *Journal of Nuclear Medicine*. 2013;54(11):1981-1988.
44. Venkatachalam TK, Pierens GK, Bernhardt PV, et al. Heteronuclear NMR Spectroscopic Investigations of Gallium Complexes of Substituted Thiosemicarbazones Including X-Ray Crystal Structure, a New Halogen Exchange Strategy, and 18F Radiolabelling. *Australian Journal of Chemistry*. 2016;69(9):1033-1048.
45. Bonnitca PD, Vāvere AL, Lewis JS, Dilworth JR. In vitro and in vivo evaluation of bifunctional bithiosemicarbazone 64Cu-complexes for the positron emission tomography imaging of hypoxia. *Journal of medicinal chemistry*. 2008;51(10):2985-2991.
46. Handley MG, Medina RA, Mariotti E, et al. Cardiac hypoxia imaging: second-generation analogues of 64Cu-ATSM. *Journal of Nuclear Medicine*. 2014;55(3):488-494.
47. John EK, Green MA. Structure-activity relationships for metal-labeled blood flow tracers: comparison of keto aldehyde bis (thiosemicarbazonato) copper (II) derivatives. *Journal of medicinal chemistry*. 1990;33(6):1764-1770.

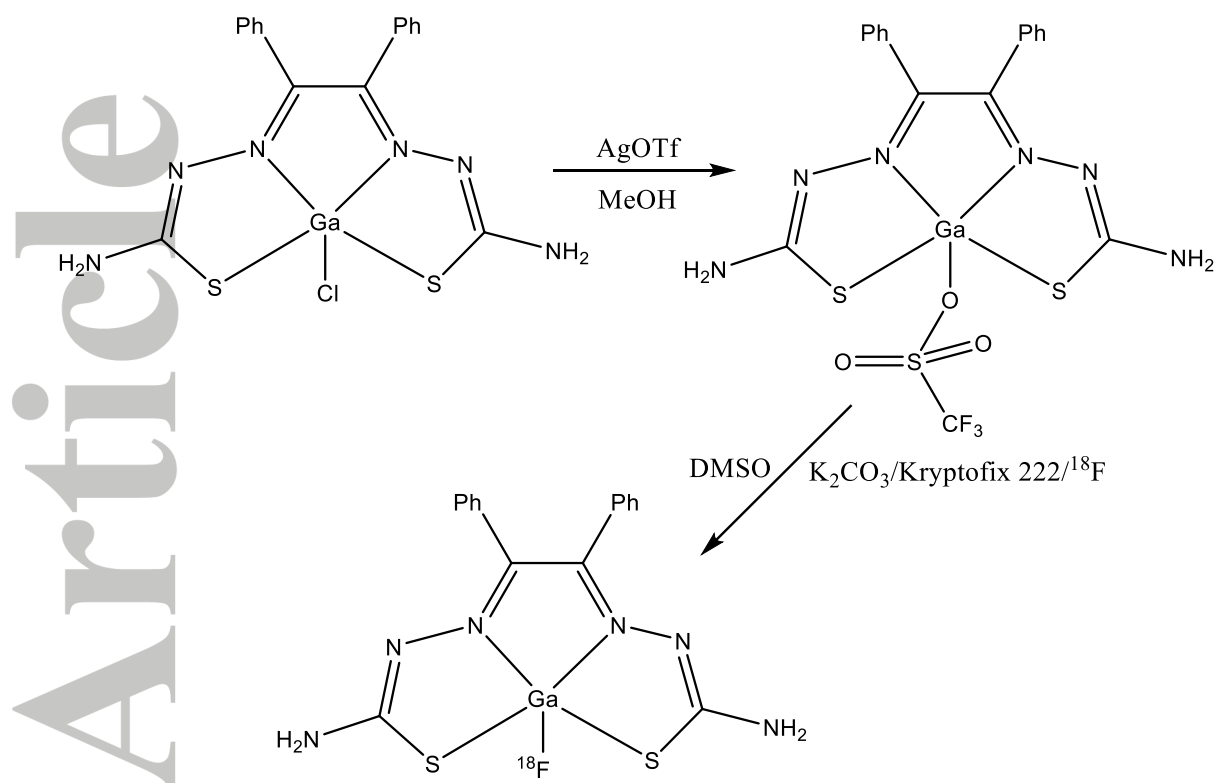
48. Green MA. A potential copper radiopharmaceutical for imaging the heart and brain: copper-labeled pyruvaldehyde bis (N4-methylthiosemicarbazone). *International Journal of Radiation Applications and Instrumentation Part B Nuclear Medicine and Biology*. 1987;14(1):59-61.
49. Chansaenpak K, Vabre B, Gabbai FP. [18F]-Group 13 fluoride derivatives as radiotracers for positron emission tomography. *Chemical Society Reviews*. 2016;45(4):954-971.



Scheme 1. Synthetic scheme for the preparation of gallium diphenyl dithiosemicarbazone complex.



Scheme 2. Radiosynthesis of ^{18}F radiolabeled diphenyl gallium dithiosemicarbazide using exchange method.



Scheme 3. Use of silver triflate as a homogenous solution exchange catalyst for introducing fluorine-18 in diphenyl gallium dithiosemicarbazone complexes.

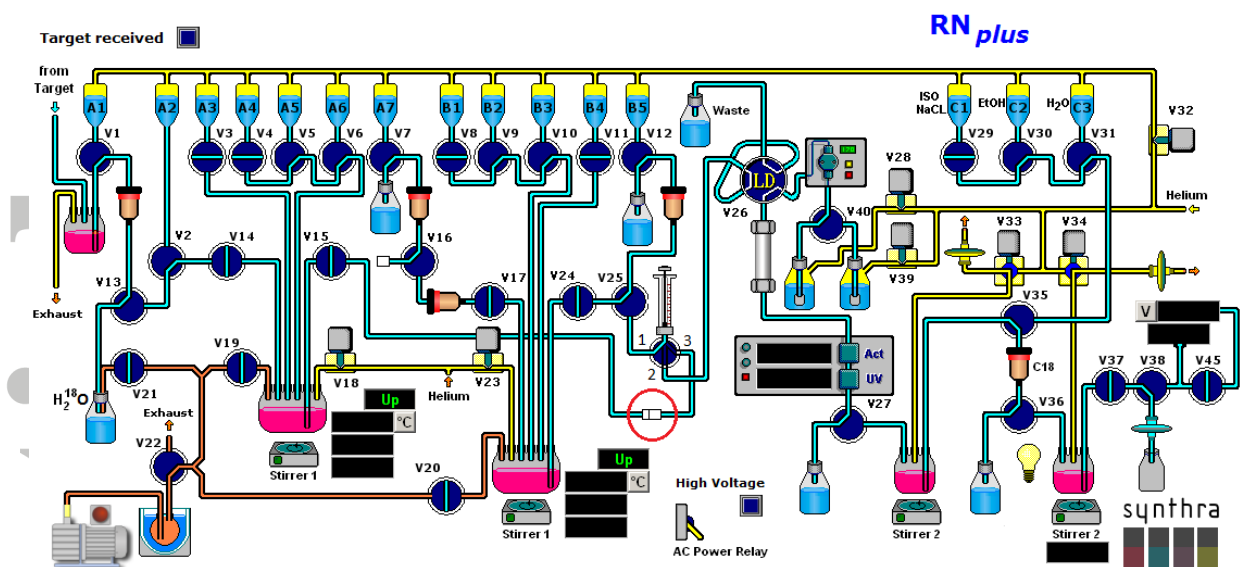


Figure 1. GUI of Synthra RN Plus automated radio-synthesis module. The fitting circled in red is manually disconnected to allow attachment of a disposable syringe containing the crude compound.

Accepted Article

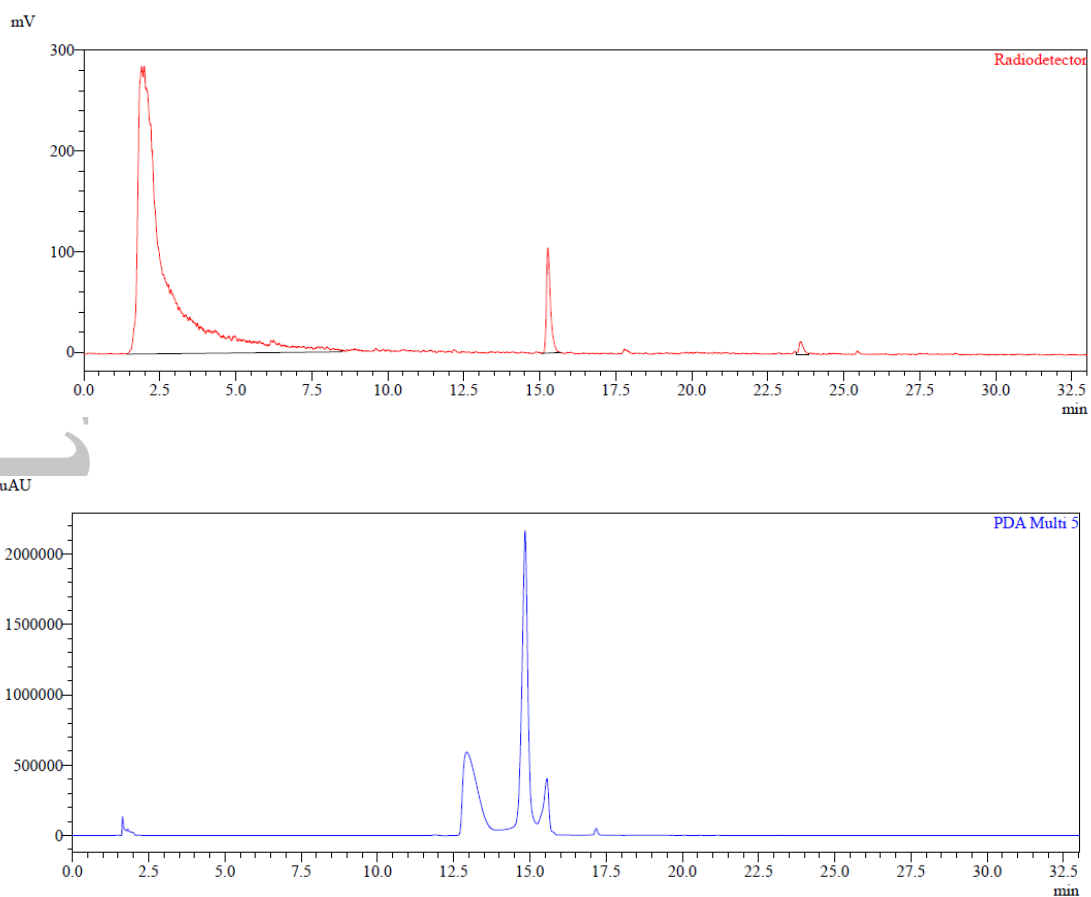


Figure 2. Analytical radio chromatogram (top) and UV chromatogram (below) of sample of crude reaction mixture. Retention time of labelled compound is ~ 15.3 minutes. Radiolabeling yield is approximately 6% based on peak areas of the radio chromatogram.

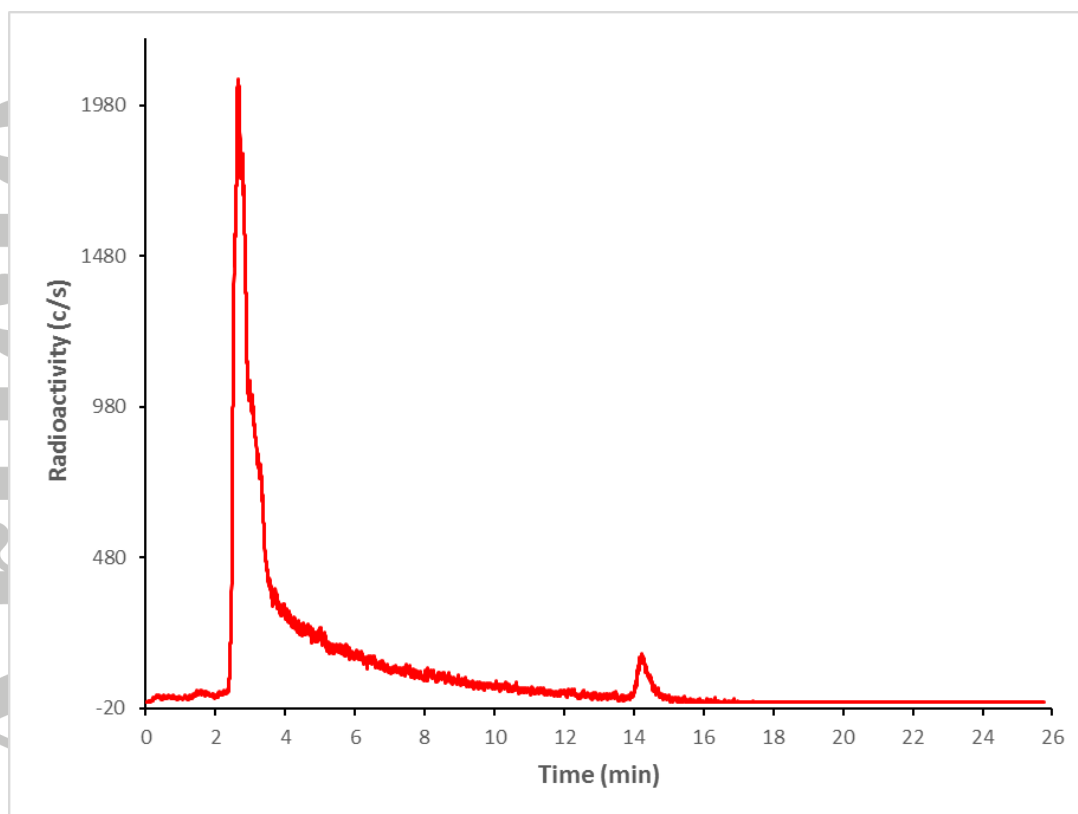


Figure 3. Semi-preparative radio chromatogram of crude reaction mixture diluted 50:50 with water. The peak at ~14 minutes was collected via valve V27 of the Synthra module for further SPE purification/reformulation.

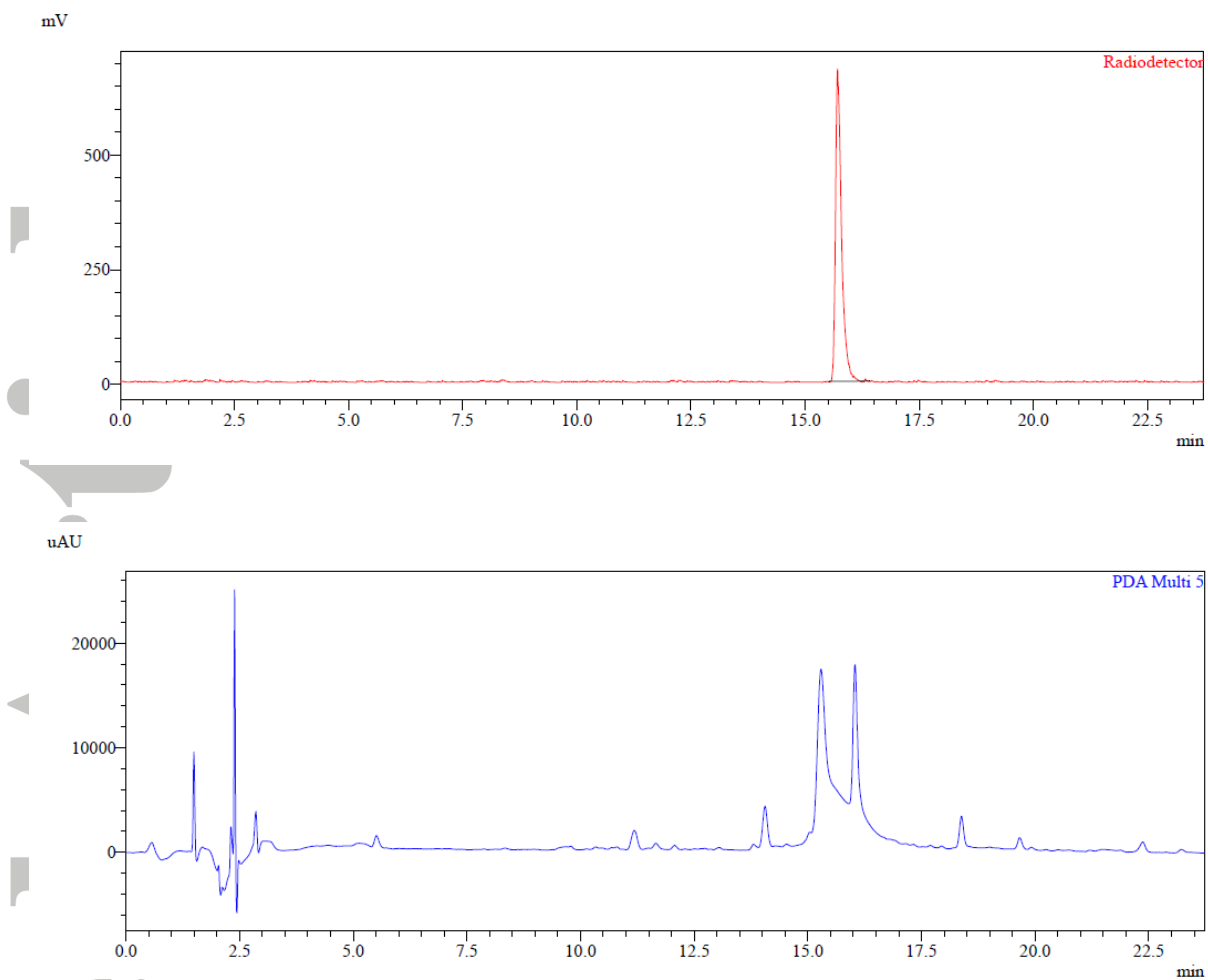


Figure 4. Analytical radio chromatogram (top) and UV chromatogram (below) of purified gallium ^{18}F -compound. Retention time of labelled compound is ~ 15.3 minutes.

Accepte

Accepted Article

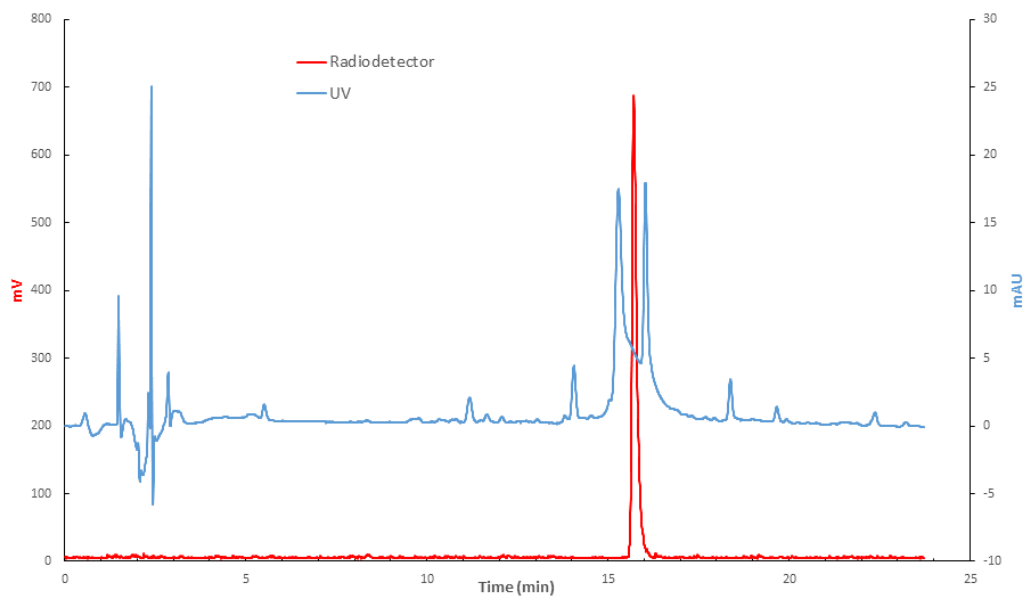


Figure 5. Analytical radio and UV chromatograms of purified gallium 18F-compound at 2.5 hours post synthesis. The Radiochemical purity remains >99% demonstrating stability. Retention time of labelled compound is ~15.3 minutes.

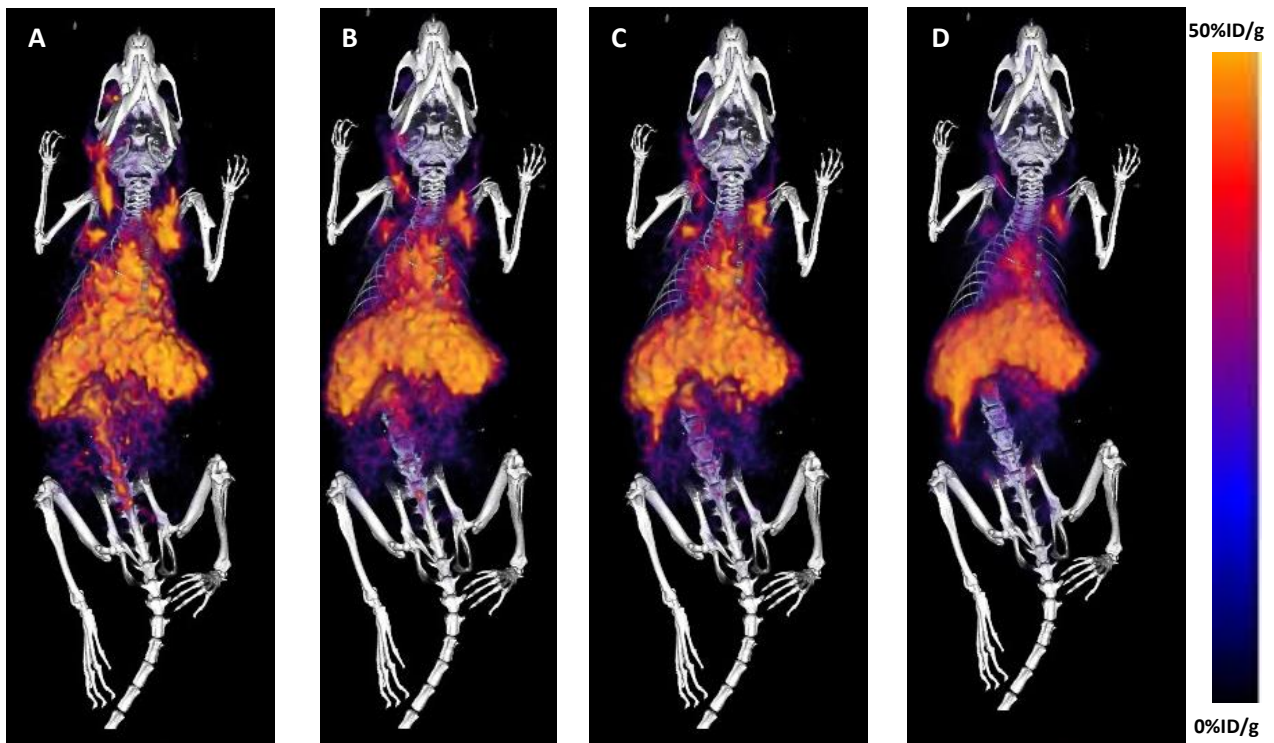


Figure 6. PET/CT Imaging of a healthy C57BL6J mouse after intravenous injection of ^{18}F -thiosemicarbazone. A: 5min, B: 15min, C: 30min, D: 60min after injection of the radiotracer.

Accepted

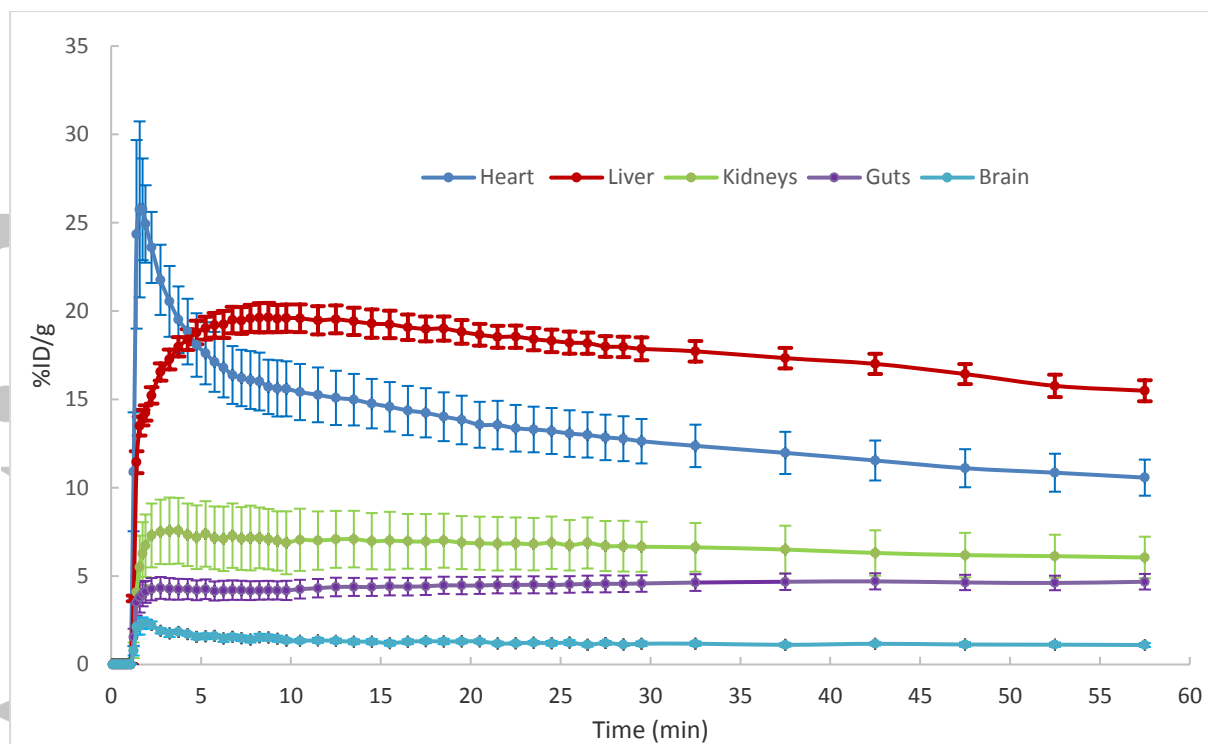


Figure 7. Time activity curve obtained from healthy C57BL6J mice injected with ^{18}F -thiosemicarbazone (Mean \pm SD, n=4)

Accepted

Table 1. Reagent quantities and radiochemical yield data. The non-purified product yield is based on the % areas of the product peak compared to the [^{18}F]F $^-$ peak of the radiochromatogram of a sample of the crude reaction mixture. The purified product yield is based on the radioactivity trapped on the C18 Solid Phase Extraction (SPE) cartridge after the semi-preparative HPLC fraction cut compared to the starting quantity of [^{18}F]F $^-$. For each experiment, the chemical precursor was dissolved in 500 μL DMSO.

K₂₂₂ (mg)	Acetonitrile (μL)	K₂CO₃ (mg)	Aqueous [^{18}F]F$^-$ (μL)	Starting Activity [^{18}F]F$^-$ (MBq)	Non-corrected Radiochemical Yield, non-purified (%)	Non-corrected Radiochemical Yield, purified (%)
1.9	500	0.35	100	4400		0.44
1.8	500	0.35	100	4400		0.77
2.1	500	0.35	100	4000		0.56
1.9	500	0.35	100	4870		0.48
1.9	500	0.35	100	2740		0.62
1.9	500	0.35	100	1720		0.78
1.9	500	0.35	25	277	5.4	1.19
2.0	500	0.35	100	148	6.1	
2.1	500	0.35	200	3100	1.3	
1.9	500	0.35	150	806	3.0	
1.9	500	0.35	100	466	4.3	
1.2	200	0.55	60	568	8.1	
1.2	200	0.57	100	740	2.2	
1.2	200	0.60	10	81	4.8	
1.3	200	0.55	15	82	5.7	

Table 2. Biodistribution 75 min after intravenous injection of ^{18}F -thiosemicarbazone in 4 healthy C57BL6J Mice. Results have been decay corrected to the time of the injection of the radiotracer and are expressed as Mean \pm Standard Deviation (SD).

	% Injected dose/organ	% Injected dose/g of organ
Heart	0.47 \pm 0.09	4.37 \pm 0.39
Lungs	0.82 \pm 0.10	4.94 \pm 0.43
Liver	16.9 \pm 3.0	18.9 \pm 3.1
Spleen	0.20 \pm 0.05	2.45 \pm 0.48
Kidneys	2.41 \pm 0.31	9.50 \pm 0.83
Gut	5.39 \pm 0.35	2.57 \pm 0.13
Brain	0.12 \pm 0.03	0.27 \pm 0.06
Blood		13.9 \pm 1.9
Muscle		1.18 \pm 0.18